Am J Physiol Heart Circ Physiol 290: H2625–H2632, 2006.
First published January 27, 2006; doi:10.1152/ajpheart.01346.2005.

Laser microdissection and pressure-catapulting technique to study gene expression in the reoxygenated myocardium

Donald E. Kuhn, Sashwati Roy, Jared Radtke, Sudip Gupta, and Chandan K. Sen

Laboratory of Molecular Medicine, Department of Surgery, Davis Heart and Lung Research Institute, The Ohio State University Medical Center, Columbus, Ohio

Submitted 21 December 2005; accepted in final form 24 January 2006

Kuhn, Donald E., Sashwati Roy, Jared Radtke, Sudip Gupta, and Chandan K. Sen. Laser microdissection and pressure-catapulting technique to study gene expression in the reoxygenated myocardium. *Am J Physiol Heart Circ Physiol* 291: H2625–H2632, 2006. First published January 27, 2006; doi:10.1152/ajpheart.01346.2005.—For focal events such as myocardial infarction, it is important to dissect infarction-induced biological responses as a function of space with respect to the infarct core. Laser microdissection pressure catapulting (LMPC) represents a recent variant of laser capture microdissection that enables robot-assisted rapid capture of catapulted tissue without direct user contact. This work represents the maiden effort to apply laser capture microdissection to study spatially resolved biological responses in myocardial infarction. Infarcted areas of the surviving ischemic-reperfused murine heart were identified using a standardized hematoxylin QS staining procedure. Standard staining techniques fail to preserve tissue RNA. Exposure of the tissue to an aqueous medium (typically used during standard immunohistochemical staining), with or without RNase inhibitors, resulted in a rapid degradation of genes, with ~80% loss in the 1st h. Tissue elements (1×10^4–4×10^6 μm^2) captured from infarcted and noninfarcted sites with micrometer-level surgical precision were collected in a chaotropic RNA lysis solution. Isolated RNA was analyzed for quality by microfluidics technology and reverse transcribed to generate high-quality cDNA. Real-time PCR analysis of the cDNA showed marked (200- and 400-fold, respectively) induction of collagen Ia and IIIa at the infarcted site compared with the noninfarcted site. This work reports a sophisticated yet rapid approach to measurement of relative gene expressions from tissue elements captured from spatially resolved microscopic regions in the heart with micrometer-level precision.

myocardial infarction; remodeling; wound healing; regenerative medicine; method

SPATIALLY RESOLVED MOLECULAR analysis of infarcted myocardial tissue has been hindered by the lack of microdissection techniques to collect tissue samples with micrometer-level precision. To address this important limitation in analytic tissue biology, laser capture microdissection (LCM) technology has been originated by the National Institutes of Health through an intensive collaboration between bioengineering and cancer pathology groups (4, 9). Under direct microscopic visualization, LCM permits rapid procurement of histologically defined tissue samples. The approach can be employed to collect pathologically defined (e.g., infarct core) tissue elements down to the resolution of a single cell. In general, in LCM, biological material is placed on a glass slide, or equivalent surface, and a thermoplastic membrane is placed in direct contact on top of the material. The laser beam source is positioned below the material, and the beam is focused through a microscope ocular lens onto the biological material on the slide. When the laser beam strikes the material, it is blasted off the glass surface and melts onto the thermoplastic membrane. The thermoplastic membrane piece containing the blasted material is then physically isolated, and the material is collected (4, 9). Laser microdissection has opened a window to new technologies. In a variant of LCM, laser microdissection and pressure catapulting (LMPC) (5), the biological material is placed directly on top of a thermoplastic [polyethylene napthalate (PEN)] membrane that covers a glass slide or equivalent. The membrane acts as a support, or scaffolding, to allow for catapulting relatively large amounts of intact material at one time. A focused laser beam is used to cut out an area of the membrane and corresponding biological material, and then the beam is defocused and the energy is used to catapult the membrane and material from the slide. A motorized stage is used to move the sample through the laser beam path to allow the user to control the size and shape of the area to be cut. The catapulted sample is generally captured in an aqueous medium positioned directly above the cut area. The major advantages of LMPC over LCM are as follows: *1*) a greater amount of tissue is captured in a given time, *2*) cellular integrity is preserved, and *3*) the biological material is obtained without direct user contact (3, 5).

LMPC enables capture of biological material ranging from defined multicellular tissue elements to specific sections of cells and organs to cellular organelles (3, 5). For the most part, LCM has been applied to the study of cancer (1, 6, 7, 13, 16, 21). Application of this technology to myocardial research has been very limited (8). An acute myocardial infarction induces ventricular remodeling, a process that can influence ventricular functions and survival outcomes (20). Animals that survive with large transmural infarctions develop heart failure without another ischemic event, as is typically seen in humans. Rodent models of myocardial infarction have been extensively studied to understand the functional, structural, and molecular changes associated with clinical ischemic heart disease (20, 27). Current treatment of myocardial infarction is directed to restoration of blood flow to the ischemic region by thrombolysis, coronary artery bypass surgery, or percutaneous transluminal coronary angioplasty. When blood flow through the myocardium is reestablished, the hibernating myocardial tissue may regain its function but may also experience additional damage and remodeling due to the reperfusion process itself (22–24). Time-dependent changes in ventricular architecture occur in

Address for reprint requests and other correspondence: C. K. Sen, Davis Heart and Lung Research Institute, 473 W. 12th Ave., Columbus, OH 43210 (e-mail: Chandan.Sen@osumc.edu).

The costs of publication of this article were defrayed in part by the payment of page charges. The article must therefore be hereby marked "*advertisement*" in accordance with 18 U.S.C. Section 1734 solely to indicate this fact.

Table 1. *Forward and reverse primer sequences, amplicon size, and location of the amplicon in the gene*

	Sequence	Size (bp)	Location (bp)
GAPDH			575–914
Forward	ATG ACC ACA GTC CAT GCC ATC ACT	339	
Reverse	TGT TGA AGT CGC AGG AGA CAA CCT	339	
Collagen Ia			1,799–1,924
Forward	GTG TGA TGG GAT TCC CTG GAC CTA	125	
Reverse	CCT GAG CTC CAG CTT CTC CAT CTT	125	
Collagen IIIa			1,998–2,148
Forward	ACC CCC TGG TCC ACA AGG ATT A	150	
Reverse	ACG TTC TCC AGG TGC ACC AGA AT	150	

the infarcted and noninfarcted regions, resulting in hypertrophy of the viable regions of the affected site (11). Tissue harvested at the infarct site via standard surgical techniques provides samples that represent a mixture of the infarcted myocardium, the peri-infarct area, and the noninfarcted myocardium. Results obtained from the molecular studies of such samples fail to provide spatially resolved information discriminating the responses in the infarcted site from those in the noninfarcted site, which may be located a few hundred micrometers away along the thickness of the muscle. LCM offers an excellent opportunity to spatially resolve molecular responses on the basis of histologically defined areas in the specimen. In this study, we developed a protocol specifically directed toward use of LMPC to study gene expression in histologically defined infarcted and noninfarcted myocardial tissue. This work presents the first account of an analytic technique that would be helpful in applying LMPC technology to the study of ventricular remodeling after myocardial infarction.

MATERIALS AND METHODS

Survival surgery for myocardial ischemia-reperfusion. Young adult (10–12 wk of age) male C57BL/6 mice (Harlan Technologies, IN) were anesthetized, held on a warm tray (37°C), and intubated endotracheally. The mice were ventilated on 100% O_2-isoflurane at an appropriate rate and tidal volume. Cardiac electrophysiology was monitored using a standard three-lead ECG setup, and changes in electrical conduction were measured using PC Powerlab software (AD Instruments). The heart was accessed via a left thoracotomy. The left lung was retracted to allow entrance to the pericardium. The left auricle was elevated to expose the coronary (left anterior descending) artery, which was isolated using 7-0 silk suture on a taper needle. The suture was secured, but not ligated, to provide for reversible ischemia via occlusion of the coronary artery. Ischemia, documented by laser-Doppler blood flow measurement, continued for 30 min after occlusion. After 30 min, the suture was released to allow for reperfusion of the injured myocardium for 7 days. On successful reperfusion, the thorax was closed with interrupted sutures, and the skin incision was closed with surgical clips. A catheter was used to aspirate the left thorax to reestablish the negative thoracic pressure and facilitate lung reexpansion (24). All animal experiment procedures were approved by the Institutional Animal Care and Use Committee of the Ohio State University.

Cardiac tissue procurement and processing. The infarction site of the heart was cut laterally, and the tissue containing the infarcted area was frozen in optimum cutting temperature compound using liquid N_2. Mouse heart samples frozen in optimum cutting temperature compound were cut into 10-μm-thick sections using a cryotome (model 3500S, Leica). The sections were placed on PEN-covered glass slides (PALM Technologies, Bernreid, Germany) and used immediately or stored at −80°C. To histologically distinguish between infarcted and noninfarcted areas, the frozen sections were stained directly with hematoxylin QS only (Vector Laboratories, Burlingame, CA). For this procedure, frozen sections were thawed for 1–2 min at room temperature, two to three drops of hematoxylin QS were added to each section, and the slides were incubated at room temperature for 1–4 min. The slides were rapidly rinsed with distilled water to remove excess stain and then allowed to air dry for 5–10 min at room temperature. The stained sections were photographed using a camera (model D30, Hitatchi) mounted on a microscope (Axiovert 200M, Zeiss). In some cases, tissue sections were stained with Masson's trichrome or hematoxylin-eosin using standard protocols.

LMPC. LMPC was performed using a PALM MicroLaser system (PALM-Zeiss, Bernreid, Germany) containing a PALM MicroBeam (driven by PALM MicroBeam software) and a PALM RoboStage and, for high-throughput sample collection, a PALM RoboMover (driven by PALM RoboSoftware version 2.2). A typical setting used for laser cutting was a beam size of 30 μm and laser strength of 30 mV under a ×10 ocular lens. Mouse heart sections were placed on PEN membrane-covered glass slides (PALM Industries) that had been treated with RNAZap (Ambion, San Antonio, TX) as instructed by the manufacturer. Sections containing the infarcted and noninfarcted areas were cut under a ×10 ocular lens and catapulted directly into 25 μl of an RNA lysis solution (RNAqueous Micro kit, Ambion).

RNA isolation and assessment of quality. RNA from LMPC samples was isolated using the RNAqueous Micro kit. The 25 μl of lysis solution used to capture the catapulted tissue in LMPC was spun into a tube, and another 75 μl of lysis solution, along with 3 μl of the supplied LCM additive and either 129 μl (to collect large and small RNA) or 52 μl (to collect >200-bp RNA) of ACS grade 100% ethanol, were added. This solution was spun through a silica-based "spin column" to bind the RNA. The columns were washed with the supplied buffers, and the RNA was eluted in two 9-μl washes using the supplied elution solution or nuclease-free distilled water. The RNA solution was then treated with DNase for 20 min at 37°C to remove DNA. The quality and approximate quantity of the resulting RNA were determined using the microfluidics system (Agilent 2100 Bioanalyzer, Agilent Technologies). In some cases, RNA quantity was verified using the RiboGreen fluorescence dye assay (Molecular Probes, Eugene, OR).

Reverse transcription. RNA isolated as described above was reverse transcribed into cDNA using the Superscript III RT kit (InVitrogen, Carlsbad, CA). For each reaction, 8 μl of the 20 μl of RNA solution were used. In some cases, the entire RNA solution was used

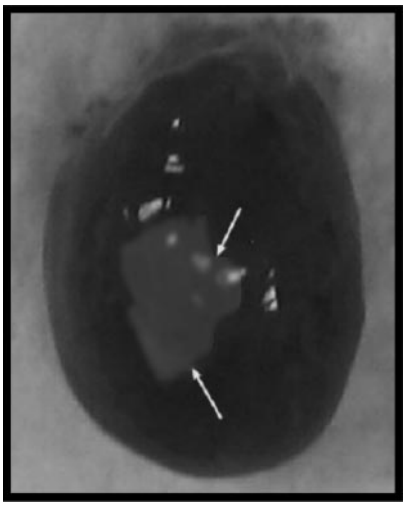

Fig. 1. Infarcted C57BL/6 mouse heart. Arrows point to a pale oval-shaped infarcted area at the surface.

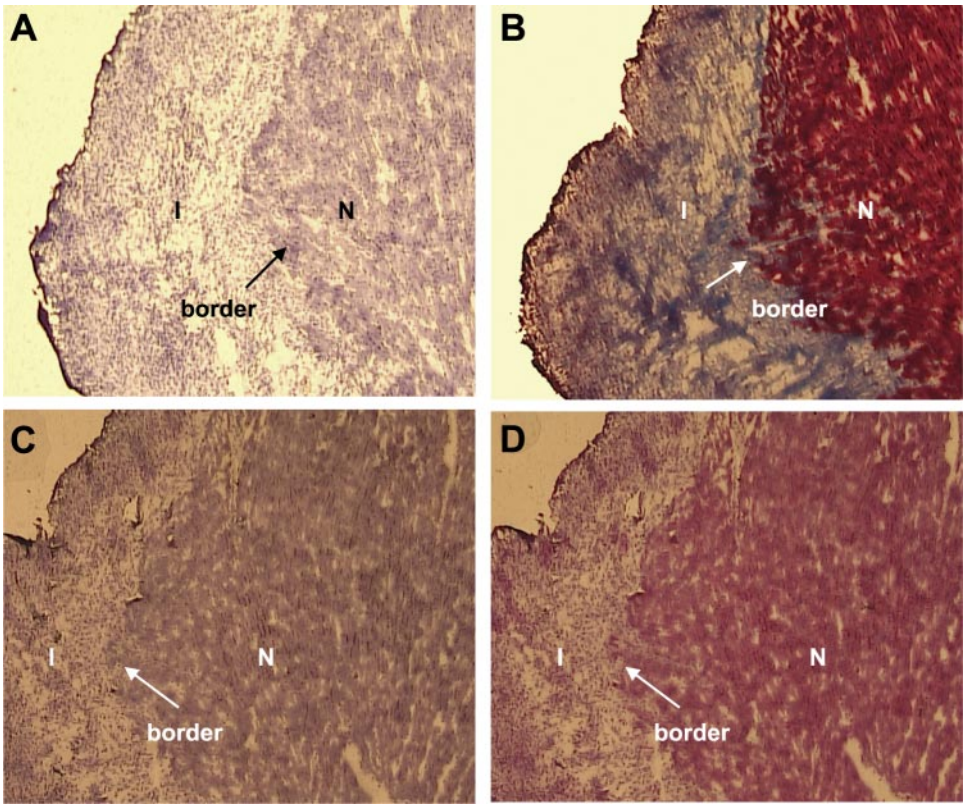

Fig. 2. Sections stained with hematoxylin, Masson's trichrome, and hematoxylin-eosin. *A* and *C*: different sections stained with hematoxylin. *B*: section corresponding to that in *A* stained with Masson's trichrome. *D*: section corresponding to that in *C* stained with hematoxylin-eosin. All 3 stains identify the same infarcted area. I, infarcted area; N, noninfarcted area. Arrow points to boundary between infarcted and noninfarcted areas.

after it was concentrated to 8 μl using a SpeedVac. Reactions were typically carried out using the supplied random hexamers. In some cases, however, the supplied oligo(dt)$_{20}$ primer was used. One microliter each of random hexamers (50 ng/μl) and dNTPs (10 mM) were added to 8 μl of RNA solution, and the resulting solution was incubated for 5 min at 65°C and then placed on ice for ≥1 min. Ten microliters of a 2× reaction mixture containing Tris·HCl (pH 7.4), 25 mM $MgCl_2$, 0.1 M dithiothreitol, 40 U of RNase Out, and 200 U of Superscript III RT were added, and the solution was incubated at 25°C for 10 min, 50°C for 50 min, and, finally, 85°C for 5 min. RNA was degraded by further incubation for 20 min at 37°C with 2 U of RNase H. The cDNA generated in RT reactions was separated on 3% agarose gels. Ethidium bromide was added directly to the sample, and electrophoresis was conducted at 125 V constant voltage.

Quantitative real-time PCR. The cDNA generated in RT reactions was used directly in real-time PCR with gene-specific primers (Table 1) using the MX3000P system (Stratagene, La Jolla, CA). The PCR included 5 μl of cDNA solution, 7.3 μl of nuclease-free distilled water, 0.1 μl of each primer solution (50 μM), and 12.5 μl of SYBR Green real-time PCR mixture (Applied Biosystems, Warrington, UK). The solution was initially incubated at 50°C for 2 min and then at 95°C for 10 min to activate the polymerase. Typically, 40 cycles with 45-s steps each were performed at 95°C, 58°C, and 72°C. The dissociation (i.e., melting) temperature (T_m) of each sample was compared with that of an included known cDNA standard to partially ensure fabrication of the correct cDNA product. The cDNA standard was also used to obtain relative quantities. GAPDH gene expression was measured to correct for differences in extraction efficiency between infarcted and noninfarcted samples. Collagen Ia and collagen IIIa gene expressions were measured to monitor our protocol, because it is well established that each is significantly increased in infarcted tissue.

Gene expression per area of tissue. Areas of 1.0×10^4 to 4×10^6 μm^2 sections were cut and captured in RNA lysis solution using LMPC as described above. The RNA was isolated and used in RT

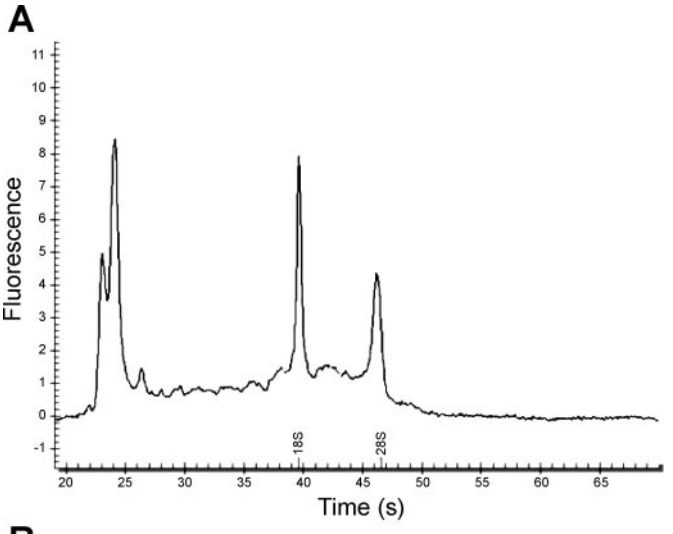

Fig. 3. *A*: electropherogram of total RNA prepared from samples obtained from mouse heart by laser microdissection and pressure catapulting (LMPC). Time scale on *x*-axis corresponds to nucleic acid length. *B*: run start and end times, peak area, and percentage of total area, along with RNA total area, concentration, and rRNA ratio (28S/18S).

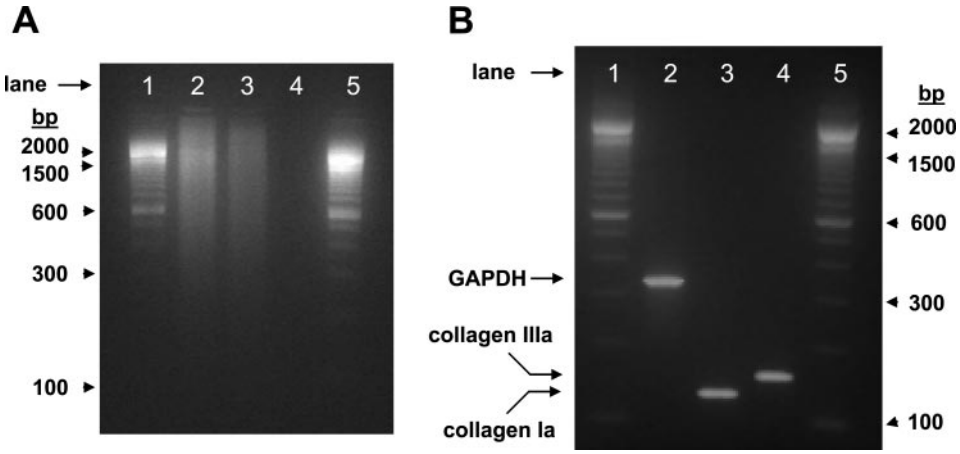

Fig. 4. Agarose gel analysis of cDNA produced in RT reactions and quantitative real-time PCR. Ethidium bromide was added directly to each sample for visualization. A 100-bp ladder is shown in *lanes 1* and *5* of each gel. *A*: cDNA from 5×10^6 μm^2 section (*lane 2*), cDNA from 2.5×10^6 μm^2 section (*lane 3*), and results from a negative control (*lane 4*). Identity of each amplicon band in *B* is listed at *left*. *Lane 2*, GAPDH amplicon product from quantitative RT-PCR; *lane 3*, collagen Ia amplicon; *lane 4*, collagen IIIa amplicon.

reactions to prepare cDNA, which was then used in quantitative RT-PCR to quantitate the expression of specific genes.

Stability in aqueous medium. For measurement of the stability of specific gene expressions in an aqueous medium, sections were incubated in PBS for various time periods. Typically, four sections were placed on each of four different PEN membrane-covered glass slides, and one slide was used for each time point. Each slide was incubated in PBS for 0, 1, 2, or 4 h in a closed moist chamber. After incubation, the slides were rinsed well with distilled water and then allowed to soak in distilled water for 1–2 min. The sections were air dried and used directly for staining, laser capture, and processing as described above. Elements corresponding to a 2.5×10^6 μm^2 area were isolated from infracted and noninfarcted tissue for use in these experiments.

Statistics. Values are means ± SD. Significance of difference between means was tested by Student's *t*-test. $P < 0.05$ was set as the threshold of significance.

RESULTS

The surgical procedure for ischemia-reperfusion resulted in a pale area of the heart, which represented the area at risk of infarction (Fig. 1). In our search for a rapid staining procedure that would histologically demarcate the infarct area, we noted that a truncated hematoxylin-eosin-staining procedure was sufficient. Heart sections subjected to the hematoxylin incubation (1–4 min) step without further treatment proved to be useful for the purposes of LMPC and subsequent genetic analyses (Figs. 2, *A* and *C*). Under the microscope (×10–×40 objective), the infarcted area was clearly discernible from the noninfarcted area: the infarcted area stained blue, and the noninfarcted area stained purple. The border between the infarcted and noninfarcted areas was clearly distinguishable and allowed for reliable identification of each area by LMPC. To verify that

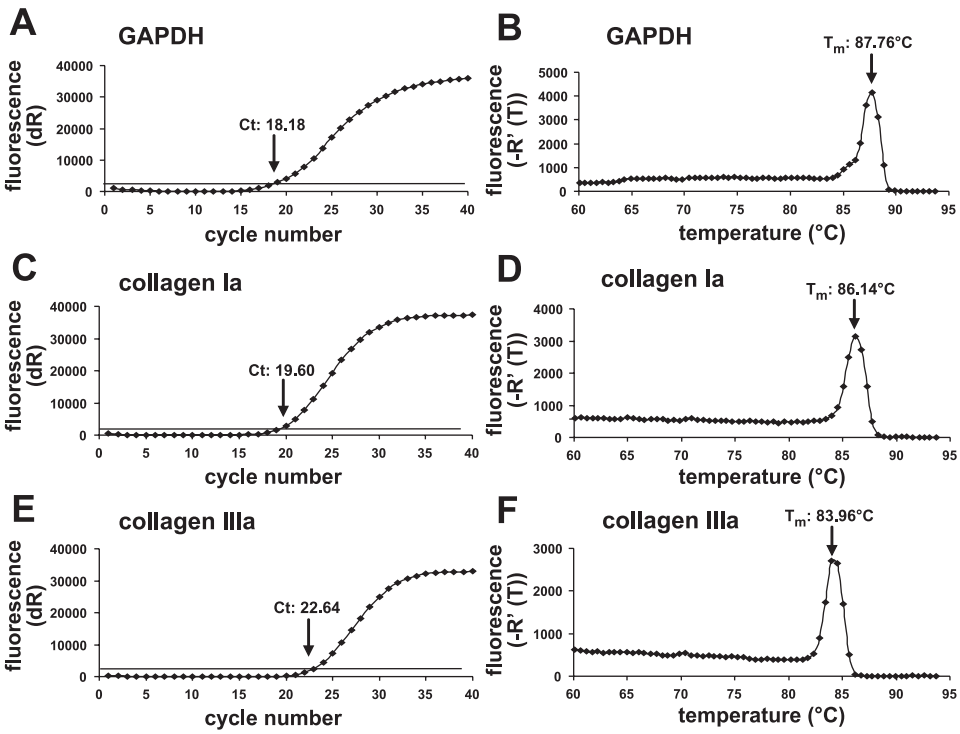

Fig. 5. Representative amplification plots (*A*, *C*, and *E*) and dissociation curves (*B*, *D*, and *F*) of quantitative RT-PCR products for GAPDH, collagen Ia, and collagen IIIa. C_t, threshold cycle; T_m, dissociation (melting) temperature. dR, baseline-corrected fluorescence; $-R'(T)$, negative first derivative of raw fluorescence.

hematoxylin staining alone accurately identified the infarcted area, sequentially cut sections from the same frozen heart were stained with Masson's trichrome (Fig. 2*B*) or the standard hematoxylin-eosin stain (Fig. 2*D*). Figure 2 illustrates that the truncated hematoxylin stain procedure was effective in accurately identifying the infarcted site, as evident by standard staining procedures such as Masson's trichrome and hematoxylin-eosin.

Quality of the RNA isolated from LMPC samples represents a major factor in determining overall success of the analytic approach. Areas of $1–4 \times 10^6$ μm^2 sections were cut and captured in RNA lysis solution. Quality of the RNA extracted from the captured tissue elements was tested using the microfluidics-based Agilent 2100 Bioanalyzer system. A typical electropherogram of RNA collected by LMPC from a 1×10^6 μm^2 section of noninfarcted heart tissue is illustrated in Fig. 3*A*. The 5S, 18S, and 28S rRNA peaks were clearly discernible. The presence of RNA over a wide range of sizes and the absence of a large peak when small degraded RNA fragments were detected indicated very little, if any, RNA degradation during sample preparation, staining, capturing, and processing. The corresponding run start and end times, area, and percentage of total area, as well as the RNA total area, concentration, and rRNA ratio are shown in Fig. 3*B*. The percentages of total area of the 18S and 28S peaks, as well as the ratio of 28S to 18S rRNA, were typical of eukaryotic cells. These results were obtained with total RNA extracts, which include all small RNA, including tRNA, small interfering RNA, and 5S rRNA. When only larger (>200-bp) RNA species were isolated, the resulting electropherogram was essentially the same as that shown in Fig. 3*A*, except the 5S peak was absent (not shown). Similar amounts of RNA were isolated from comparably sized areas of infarcted and noninfarcted tissue. The yield in our procedure was 9.6 ± 0.99 fg RNA/μm^2 on the basis of RNA concentrations reported by the Agilent 2100 Bioanalyzer system.

The cDNA produced in RT reactions of RNA from mouse hearts was separated on 3% agarose gels, and the results are shown in Fig. 4*A, lanes 1* and *2*. The presence of 200- to >2,000-bp cDNA species in each lane is shown by the even distribution of cDNA over this size range. No evidence of degradation was noted. These results indicate that our procedure resulted in high-quality cDNA. The cDNA produced in RT reactions of tissue extracts from infarcted and noninfarcted areas was subjected to quantitative real-time PCR using the gene-specific primers listed in Table 1. Figure 4*B* shows that a single amplicon of the expected size was produced in these reactions for all three primer pairs tested. Examples of amplification plots and dissociation curves for each of these primer sets are shown in Fig. 5. Figure 5*A* shows that detection of GAPDH gene product in the given example occurred at ~18 cycles, typical of what is generally reported in the literature (10, 12). Collagen IIIA was detected at ~20 cycles and collagen IA at ~22 cycles. The dissociation of each of the specific cDNA products occurs at a specific and unique T_m, which is shown in Fig. 5 for GAPDH, collagen Ia, and collagen IIIa. These T_m values were identical to the control cDNA values.

The minimal area of tissue section, or element, required to measure GAPDH, collagen Ia, and collagen IIIa gene expression was determined (Fig. 6). A linear relation was observed between element area and expression of these genes (Fig. 6). All three genes were reliably quantified from a section as small as 1.0×10^4 μm^2. The stability of specific genes in aqueous medium was tested (Fig. 7). Under such conditions, the genes were highly unstable: ~80% of each gene was lost within the 1st h. The results were similar for each gene, whether the tissue was from an infarcted or a noninfarcted area (Fig. 7). RNase inhibitors, such as RNaseOut (InVitrogen) and SuperaseIN (Ambion), did not prevent the loss of genes when samples were held in aqueous medium. Using the procedure described here, we noted that expression of collagen Ia as well as collagen IIIa was markedly (400- and 200-fold, respectively) higher at the infarcted site 7 days after infarction than in noninfarcted tissue (Fig. 8). An overview of the procedure developed in this study is presented in Fig. 9.

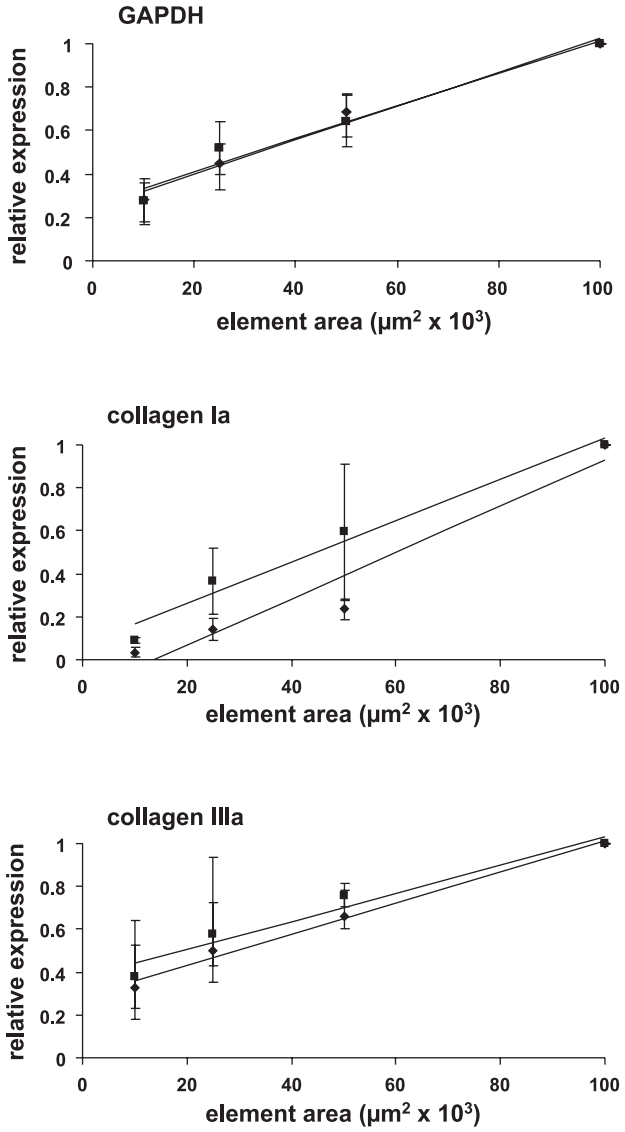

Fig. 6. LMPC-captured element area vs. GAPDH (*A*), collagen Ia (*B*), and collagen IIIa (*C*) gene expression. For normalization of GAPDH, collagen Ia, and collagen IIIa values, value of 1×10^5 μm^2 sample was set to 1.0 and lower values were scaled accordingly. Values are means ± SD. Trend lines correspond to values from infarcted (◆) and noninfarcted tissues (■).

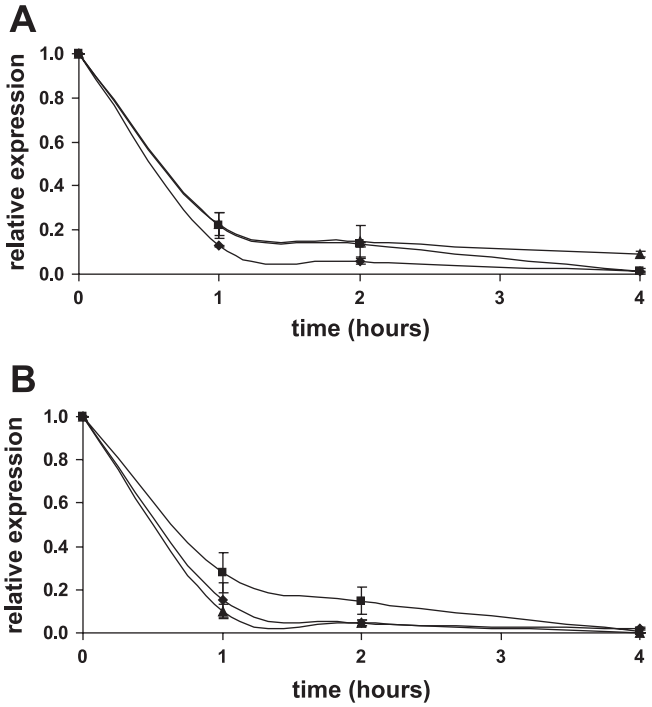

Fig. 7. Stability of GAPDH (◆), collagen Ia (■), and collagen IIIa (▲) gene expression as a function of duration of exposure to aqueous medium. *A*: infarcted tissue. *B*: noninfarcted tissue. For normalization, relative value was set at 0–1.0 h and values were scaled. Values are means ± SD.

DISCUSSION

Ischemia in the heart results in a hypoxic area containing a central focus of near-zero P_{O_2} bordered by tissue with diminished but nonzero P_{O_2} (26). These border zones extend for several millimeters from the hypoxic core, with the P_{O_2} progressively increasing from the focus to the normoxic region (25). Thus reperfusion with O_2-rich blood results in the highest ΔP_{O_2} at the core of the infarction, resulting in reoxygenation injury. The ΔP_{O_2} at the peri-infarct region is not as high, however. Here, reoxygenation triggers a remodeling response by inducing the differentiation of cardiac fibroblasts to myofibroblasts (22–24). For focal events, such as myocardial infarction, it is important to dissect infarction-induced biological responses as a function of space. For example, it is important to precisely discriminate the events at the core of infarction from those at the periphery or the peri-infarct region. Development of such understanding requires micrometer-level reso-

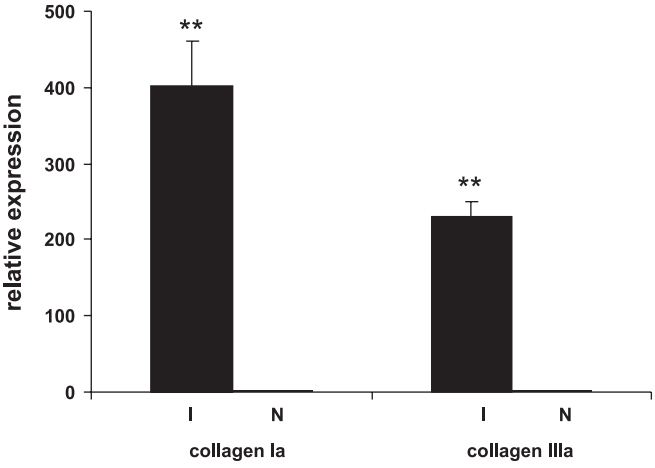

Fig. 8. Expression of collagen Ia and collagen IIIa genes at infarcted (I) site relative to noninfarcted (N) site on the same section of mouse heart. Values are means ± SD. **Significantly higher than noninfarcted site, $P < 0.0001$.

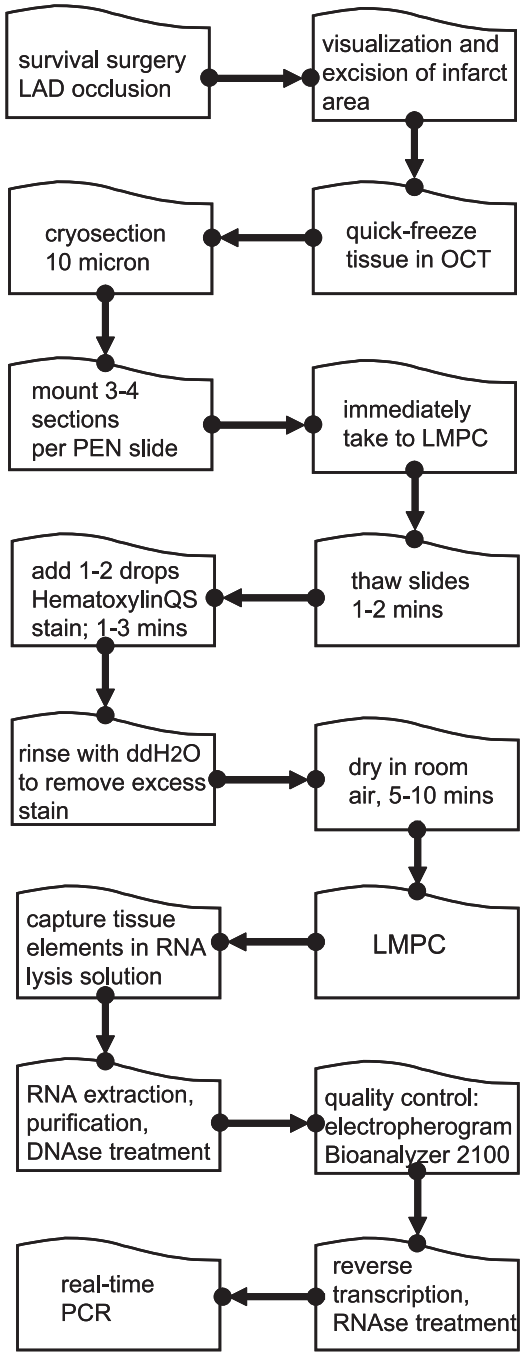

Fig. 9. Summarized protocol for determination of gene expression from LMPC tissue elements captured from infarcted or noninfarcted site in a mouse heart section. Frozen blocks of tissue were sectioned, cDNA was prepared from histologically defined infarcted or noninfarcted sites, and specific gene expression was analyzed in <1 working day. ddH_2O, double-distilled water; PEN, polyethylene naphthalate; OCT, optimum cutting temperature compound; LAD, left anterior descending coronary artery.

lution of the surgical procedure for tissue collection. LMPC offers such capability.

LMPC of tissue sections from the infarcted areas rests on the capability to rapidly and reliably distinguish infarcted and noninfarcted sites under the microscope. Although several standard staining procedures have been optimized for that purpose, these techniques are not suitable for LMPC, because they take too much time, allowing degradation of nucleic acids. Histological stains such as Masson's trichrome and hematoxylin-eosin, as well as immunohistochemical approaches, have been widely used to identify the infarcted myocardial tissue. Masson's trichrome exposes the tissue sections to harsh chemicals and is not rapid. Hematoxylin-eosin also requires many steps and exposes the sections to ethanol and xylene. During standard immunohistochemical approaches, prolonged exposure of the tissue sections to an aqueous medium poses the risk of RNA degradation. Our results showed that 80% of the mRNA is lost during the 1st h under such conditions. In this study, we have optimized a truncated hematoxylin-eosin staining procedure that is capable of reliably demarcating the infarcted vs. noninfarcted areas. Employing this approach, one may go from frozen heart blocks to laser capture from sections in $<$20 min.

The integrity and quality of the RNA isolated from the laser-captured tissue are centrally important to ensure accurate quantification of gene expression (15, 19). The advantages of the LMPC approach for laser capture include rapid automated microdissection and no direct user contact with the sample. Typically, one slide with three or four sections produced 3–5 $\times$ 10^6 μm^2 of infarct-tissue material. Cutting, catapulting, and capturing of this amount of cellular material from infarcted and noninfarcted tissue can be accomplished in $<$1 h. The use of chaotropic RNA lysis solution helps preserve RNA integrity (2). We utilized that approach to collect catapulted tissue elements.

The minimal amount of LMPC-collected tissue required in this protocol to obtain gene products from quantitative RT-PCR was 1.0 $\times$ 10^4 μm^2. This small amount of tissue can be collected in a matter of minutes from a single section. The RNA yield obtained from the tissue elements lends itself to several real-time PCR assays. We have assayed for three genes from 1.0 $\times$ 10^4 μm^2 tissue. Because we typically obtained 1 $\times$ 10^6 μm^2 of infarct tissue from one 10-μm tissue section, the resulting RNA is sufficient for 300 real-time PCR assays. Also, because gene expressions can be measured linearly up to $\geq$4 $\times$ 10^6 μm^2 of tissue, time can be saved by collecting this amount together and then dividing the cDNA for multiple gene expression measurements.

Immunohistochemistry represents a common technique for the identification of tissue components within sections mounted on glass slides for use in laser capture studies (17). Once identified by immunohistochemistry, the desired samples are collected using laser capture, with one common purpose being to extract RNA and eventually analyze the expression of specific genes. However, we noted that, even in the presence of RNase inhibitors over the time period of a typical immunohistochemical procedure, the measurable quantity of gene in an aqueous medium significantly decreased. These results indicate the need for specific histological approaches to serve the needs of gene expression assay from laser-captured material.

The extracellular matrix is a key component in the postinfarction remodeling process, and increases in collagen in the infarcted area replace necrotic myocytes and form a scar. In the myocardium, collagen represents the most abundant structural protein of the connective tissue network. Its structural organization consists of a complex weave of collagen fibers that surrounds and interconnects myocytes, groups of myocytes, muscle fibers, and muscle bundles. The myocardial healing response is characterized by the deposition of type I and III collagen (14, 18). Collagen is the major extracellular matrix protein in the heart and represents a crucial target for antiremodeling and cardioprotective therapy (28). Consistent with previous reports, our LMPC approach showed that collagen I and collagen III are strikingly (2 orders of magnitude) induced in response to myocardial infarction. This work reports a sophisticated approach to measure relative gene expressions from tissue elements captured from spatially resolved microscopic regions in the heart. The procedure provides high-quality RNA and cDNA that can be used to measure specific gene expressions using qualitative real-time PCR.

GRANTS

This work was supported by National Heart, Lung, and Blood Institute Grant RO1 HL-073087 to C. K. Sen.

REFERENCES

1. **Ai J, Tan Y, Ying W, Hong Y, Liu S, Wu M, Qian X, and Wang H.** Proteome analysis of hepatocellular carcinoma by laser capture microdissection. *Proteomics* 6: 538–546, 2006.
2. **Alexander RJ and Raicht RF.** Purification of total RNA from human stool samples. *Dig Dis Sci* 43: 2652–2658, 1998.
3. **Bazan V, La Rocca G, Corsale S, Agnese V, Macaluso M, Migliavacca M, Gregorio V, Cascio S, Sisto PS, Di Fede G, Buscemi M, Fiorentino E, Passantino R, Morello V, Tomasino RM, and Russo A.** Laser pressure catapulting (LPC): optimization LPC-system and genotyping of colorectal carcinomas. *J Cell Physiol* 202: 503–509, 2005.
4. **Bonner RF, Emmert-Buck M, Cole K, Pohida T, Chuaqui R, Goldstein S, and Liotta LA.** Laser capture microdissection: molecular analysis of tissue. *Science* 278: 1481–1483, 1997.
5. **Burgemeister R.** New aspects of laser microdissection in research and routine. *J Histochem Cytochem* 53: 409–412, 2005.
6. **Chang MC, Chang YT, Tien YW, Sun CT, Wu MS, and Lin JT.** Distinct chromosomal aberrations of ampulla of Vater and pancreatic head cancers detected by laser capture microdissection and comparative genomic hybridization. *Oncol Rep* 14: 867–872, 2005.
7. **Chew K, Rooney PH, Cruickshank ME, and Murray GI.** Laser capture microdissection and PCR for analysis of human papilloma virus infection. *Methods Mol Biol* 293: 295–300, 2005.
8. **Chimenti C, Russo A, Pieroni M, Calabrese F, Verardo R, Thiene G, Russo MA, Maseri A, and Frustaci A.** Intramyocyte detection of Epstein-Barr virus genome by laser capture microdissection in patients with inflammatory cardiomyopathy. *Circulation* 110: 3534–3539, 2004.
9. **Emmert-Buck MR, Bonner RF, Smith PD, Chuaqui RF, Zhuang Z, Goldstein SR, Weiss RA, and Liotta LA.** Laser capture microdissection. *Science* 274: 998–1001, 1996.
10. **Fassunke J, Majores M, Ullmann C, Elger CE, Schramm J, Wiestler OD, and Becker AJ.** In situ-RT and immunolaser microdissection for mRNA analysis of individual cells isolated from epilepsy-associated glioneuronal tumors. *Lab Invest* 84: 1520–1525, 2004.
11. **Gidh-Jain M, Huang B, Jain P, Gick G, and El-Sherif N.** Alterations in cardiac gene expression during ventricular remodeling following experimental myocardial infarction. *J Mol Cell Cardiol* 30: 627–637, 1998.
12. **Goldsworthy SM, Stockton PS, Trempus CS, Foley JF, and Maronpot RR.** Effects of fixation on RNA extraction and amplification from laser capture microdissected tissue. *Mol Carcinog* 25: 86–91, 1999.
13. **Guo J, Colgan TJ, DeSouza LV, Rodrigues MJ, Romaschin AD, and Siu KW.** Direct analysis of laser capture microdissected endometrial carcinoma and epithelium by matrix-assisted laser desorption/ionization mass spectrometry. *Rapid Commun Mass Spectrom* 19: 2762–2766, 2005.

14. **Kawahara E, Mukai A, Oda Y, Nakanishi I, and Iwa T.** Left ventriculotomy of the heart: tissue repair and localization of collagen types I, II, III, IV, V, VI and fibronectin. *Virchows Arch* 417: 229–236, 1990.
15. **Kerman IA, Buck BJ, Evans SJ, Akil H, and Watson SJ.** Combining laser capture microdissection with quantitative real-time PCR: effects of tissue manipulation on RNA quality and gene expression. *J Neurosci Methods.* 2005 Dec 5 [Epub ahead of print].
16. **Lawrie LC and Curran S.** Laser capture microdissection and colorectal cancer proteomics. *Methods Mol Biol* 293: 245–253, 2005.
17. **Lindeman N, Waltregny D, Signoretti S, and Loda M.** Gene transcript quantitation by real-time RT-PCR in cells selected by immunohistochemistry-laser capture microdissection. *Diagn Mol Pathol* 11: 187–192, 2002.
18. **Omura T, Yoshiyama M, Takeuchi K, Hanatani A, Kim S, Yoshida K, Izumi Y, Iwao H, and Yoshikawa J.** Differences in time course of myocardial mRNA expression in non-infarcted myocardium after myocardial infarction. *Basic Res Cardiol* 95: 316–323, 2000.
19. **Perez-Novo CA, Claeys C, Speleman F, Van Cauwenberge P, Bachert C, and Vandesompele J.** Impact of RNA quality on reference gene expression stability. *Biotechniques* 39: 52, 54, 56, 2005.
20. **Pfeffer MA, Pfeffer JM, Fishbein MC, Fletcher PJ, Spadaro J, Kloner RA, and Braunwald E.** Myocardial infarct size and ventricular function in rats. *Circ Res* 44: 503–512, 1979.
21. **Pijuan L, Vicioso L, Bellosillo B, Ferrer MD, Baro T, Pedro C, Lloreta-Trull J, Munne A, and Serrano S.** CD20-negative T-cell-rich B-cell lymphoma as a progression of a nodular lymphocyte-predominant Hodgkin's lymphoma treated with rituximab: a molecular analysis using laser capture microdissection. *Am J Surg Pathol* 29: 1399–1403, 2005.
22. **Roy S, Khanna S, Bickerstaff AA, Subramanian SV, Atalay M, Bierl M, Pendyala S, Levy D, Sharma N, Venojarvi M, Strauch A, Orosz CG, and Sen CK.** Oxygen sensing by primary cardiac fibroblasts: a key role of $p21^{Waf1/Cip1/Sdi1}$. *Circ Res* 92: 264–271, 2003.
23. **Roy S, Khanna S, and Sen CK.** Perceived hyperoxia: oxygen-regulated signal transduction pathways in the heart. *Methods Enzymol* 381: 133–139, 2004.
24. **Roy S, Khanna S, Wallace WA, Lappalainen J, Rink C, Cardounel AJ, Zweier JL, and Sen CK.** Characterization of perceived hyperoxia in isolated primary cardiac fibroblasts and in the reoxygenated heart. *J Biol Chem* 278: 47129–47135, 2003.
25. **Rumsey WL, Pawlowski M, Lejavardi N, and Wilson DF.** Oxygen pressure distribution in the heart in vivo and evaluation of the ischemic "border zone." *Am J Physiol Heart Circ Physiol* 266: H1676–H1680, 1994.
26. **Sen CK, Khanna S, and Roy S.** Perceived hyperoxia: oxygen-induced remodeling of the reoxygenated heart. *Cardiovasc Res* 2006 Feb 14 [EPub ahead of print].
27. **Stanton LW, Garrard LJ, Damm D, Garrick BL, Lam A, Kapoun AM, Zheng Q, Protter AA, Schreiner GF, and White RT.** Altered patterns of gene expression in response to myocardial infarction. *Circ Res* 86: 939–945, 2000.
28. **Zannad F and Radauceanu A.** Effect of MR blockade on collagen formation and cardiovascular disease with a specific emphasis on heart failure. *Heart Fail Rev* 10: 71–78, 2005.